

# OPTIMIZING Pb BEAM LOSSES AT THE LHCb FOR MAXIMUM LUMINOSITY

A. Frasca\*, R. Bruce, F. Cerutti, CERN, Geneva, Switzerland

A. Ciccotelli, University of Manchester, Manchester, UK and CERN, Geneva, Switzerland

M. Patecki, Warsaw University of Technology, Warsaw, Poland

## Abstract

In addition to the physics program with proton beams, the Large Hadron Collider (LHC) at CERN also provides collisions of fully-stripped Pb beams for about one month per year. When colliding Pb nuclei, electromagnetic interactions are the dominating processes because of the intense Coulomb field produced by the ions. These ‘ultra-peripheral’ interactions give rise to ions with a changed magnetic rigidity. This causes losses in the machine that can impose limits on the luminosity. Among them, the bound-free pair production (BFPP) causes a localised power deposition downstream of each collision point, which could induce superconducting magnet quenches if not well controlled. These losses were studied and successfully mitigated for most LHC experiments, however the recent request by LHCb to increase the Pb-Pb luminosity requires a revision of BFPP collisional loss limitations. In this paper, the simulation of BFPP losses from Pb-Pb collisions around LHCb is presented. The loss patterns are discussed for different beam parameters. Finally, a mitigation strategy by means of an orbit bump is studied.

## INTRODUCTION

Each operational year, for about one month, the Large Hadron Collider (LHC) [1] is operated as a heavy-ion collider. Two beams (B1 and B2) of fully-stripped  $^{208}\text{Pb}^{+82}$  ions are accelerated up to top energy<sup>1</sup> and brought into collision at the experiments ATLAS, ALICE, CMS and LHCb (at the interaction points IP1, IP2, IP5 and IP8). So far, four Pb-Pb runs have been executed [2–5], and more are foreseen in the incoming years [6, 7].

During Pb-Pb operation, the ultraperipheral electromagnetic interactions for colliding nuclei with an impact parameter<sup>2</sup>  $b > 2R$ , where  $R$  is the nucleus radius, dominate over the nuclear inelastic interactions ( $b < 2R$ ). They are responsible of two main effects: i) lepton pair production in collisions between quasireal photons and ii) emissions of nucleons in electromagnetic dissociation (EMD) [8]. In contrast to the innocuous free pair production, in (single) bound-free pair production (BFPP) one electron is created in a bound state of one ion:



\* alessandro.frasca@cern.ch

<sup>1</sup> Previously 6.37 Z TeV was achieved, the upcoming run aims at 6.8 Z TeV and the design energy is 7 Z TeV.

<sup>2</sup> The impact parameter  $b$  is defined as the perpendicular distance between the path of a projectile and the center of a potential field created by an object that the projectile is approaching.

Both BFPP and EMD cause a very small transverse momentum recoil but a well-defined magnetic rigidity change, giving rise to narrow secondary beams. They follow a dispersive trajectory and could eventually hit the aperture, causing a localised power deposition given by

$$P_p = \mathcal{L} \sigma_p E_b , \quad (2)$$

where  $\mathcal{L}$  is the luminosity,  $\sigma_p$  is the interaction cross section and  $E_b$  is the beam energy. The induced beam losses risk triggering beam dumps or magnet quenches, which gave rise to luminosity limitations in previous runs [8–12].

Among these processes, BFPP has by far the highest cross section (281 b [10]): it is the most dangerous process and hence this paper will focus only on it. Mitigation measures for BFPP consist of orbit bumps to deflect the BFPP beams to a safer impact location and carefully dispose of resulting losses [8]. The above measures have been adopted at every IP [6, 8] except at IP8, where luminosity levelling to a safe value of  $10^{27} \text{ cm}^{-2}\text{s}^{-1}$  remained the only option, compatible with previous LHCb luminosity requirements.

Because of a recent request to increase the integrated LHCb luminosity until the end of LHC Run 4 [6, 7], an alleviation strategy should be studied to allow also in LHCb a higher peak luminosity. In this paper we present the results of these studies. For the first time, a full study of the BFPP losses at LHCb, based on SixTrack simulations, is conducted. It consists of the tracking of BFPP particles emerging from IP8 and the analysis of their resulting loss pattern. Finally, a partial mitigation strategy through orbit bumps is proposed.

## MITIGATION STRATEGIES FOR BFPP

**ATLAS and CMS** The optics around IP1 and IP5 are similar, thus allowing a common analysis for the two experiments. BFPP beams emerging from either ATLAS or CMS naturally hit the second superconducting dipole of cell 11 of the dispersion suppressor (DS)<sup>3</sup> [8]. Since an empty connection cryostat is located in cell 11, it is possible to move the losses out of the dipole MB.B11 into that connection cryostat by means of an horizontal orbit bump around the impact location [10]. The higher steady-state quench limit of bus bars in the connection cryostat ( $200\text{--}300 \text{ mW/cm}^3$ ) than in dipole magnets ( $10\text{--}20 \text{ mW/cm}^3$ ), as well as the geometric placement of the superconductors, ensure a greatly reduced risk of

<sup>3</sup> The DS is the transition region connecting the FODO cells in the arcs to both sides of the straight sections hosting the experiments with the function of suppressing the dispersion at the IP. It is made up of four cells, numbered from 8 to 11, with each one containing one superconducting quadrupole and two superconducting dipoles.

quench and therefore a complete alleviation of the limits for presently achievable luminosities [8]. This measure has been adopted at both IP1 and IP5 since Run 2 (2015), enabling to exceed a peak luminosity of  $6 \times 10^{27} \text{ cm}^{-2}\text{s}^{-1}$  [12].

**ALICE** Around IP2, the quadrupoles have opposite polarity with respect to those around IP1/5 and this does not permit implementing the same strategy. BFPP beams emerging from ALICE hit the second superconducting dipole of the cell 10, MB.B10. Since the dispersion function, and hence the BFPP trajectory, has a minimum at the location of the connection cryostat, there is no possibility to move the losses there with an orbit bump. During 2015 and 2018 runs, the luminosity of ALICE was levelled to  $10^{27} \text{ cm}^{-2}\text{s}^{-1}$  to keep BFPP power deposition below the quench limit. In order to achieve a peak luminosity in Run 3 similar to that of ATLAS and CMS, new dispersion suppressor collimators, called TCLDs, were installed in the connection cryostats around ALICE during Long Shutdown 2 (LS2) within the framework of the High-Luminosity LHC Project [13], enabling a factor 6 higher peak luminosity following a recent ALICE upgrade. The TCLDs can safely intercept the BFPP losses when the beams are deflected by a horizontal orbit bump around the quadrupole Q10 [14].

**LHCb** The optics around IP8 is similar to that around IP2, hence not allowing to move BFPP losses into the connection cryostat through a horizontal orbit bump. TCLD collimators, as used for ALICE, would be a viable alleviation but such an upgrade is presently not foreseen. The BFPP losses around IP8 as well as potential alternative mitigations are studied in the following.

## SIMULATION SETUP

The following study was carried out using the MAD-X code [15], which has many different functionalities for particle accelerator design, and the 6D single particle tracking code SixTrack [16–19], which also includes particle-matter interactions in the collimation system. SixTrack allows to simulate the distribution of the beam losses around the ring by tracking an initial particle distribution. In the following simulations, both the 2018 LHC heavy-ion optics and beam parameters (6.37 Z TeV energy, emittance of  $2.3 \mu\text{m}$ , 1.1 ns bunch length) [5, 20] and the design ones (7 Z TeV energy,  $1.6 \mu\text{m}$  emittance, 1.1 ns bunch length) [6] have been considered.

## BFPP BEAM TRACKING FROM IP8

SixTrack was used to track BFPP particles from IP8 in both B1 and B2, computing the resulting loss patterns. The dispersive trajectory of BFPP  $^{208}\text{Pb}^{+81}$  ions has been mimicked by tracking fully stripped  $^{208}\text{Pb}^{+82}$  ions with an effective fractional momentum offset  $\delta = \frac{1}{81}$ , corresponding to the magnetic rigidity change from the extra electron. The momentum and angular kicks from the interaction are very small and were neglected. The initial spatial distribution of

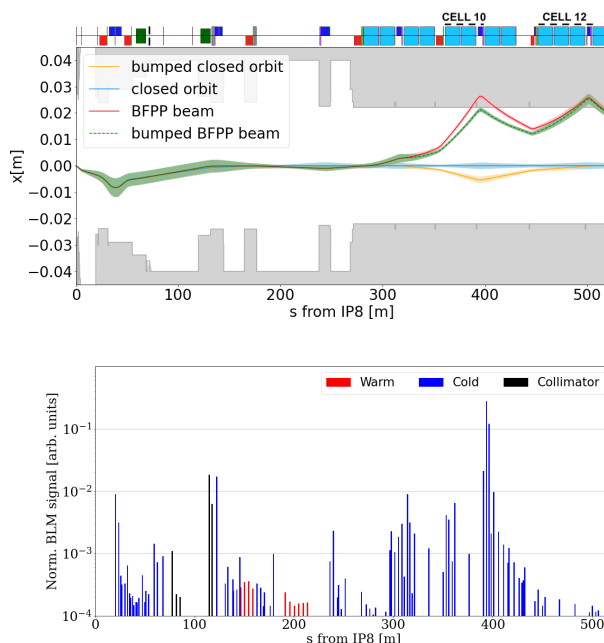


Figure 1: Top: Trajectories on the horizontal plane computed by MAD-X with and without orbit bump for B1 ( $3\sigma$  envelopes), with the machine aperture shown in grey. Bottom: LHC Beam loss monitor signals from physics operation in 2018 (fill #7477).

the colliding ions is narrower than the beam distributions by a factor  $\sqrt{2}$  [10]. For each case an initial Gaussian distribution of  $10^4$  ions was tracked. The momentum spread was neglected, which results in conservative and narrower estimations of the loss patterns.

The results show that the BFPP beams hit the superconducting dipoles MB.B10R8.B1 and MB.B10L8.B2, around the  $s$ -coordinates 386.4 m and 365.2 m from IP8, on the two sides respectively. The RMS size the BFPP loss longitudinal distributions are shown in Table 1. The  $s$ -positions have been compared to logged measurements from beam loss monitors (BLMs) in a typical 2018 Pb-Pb fill (see Fig. 1, showing B1—a qualitatively similar situation is found for B2). In general, a very good agreement was found for the BFPP loss location, i.e. the highest blue bar in the measurement, although the highest measured BLM signals were found slightly downstream of the simulated locations ( $\sim 7$  m for B1 and  $\sim 5$  m for B2). This can be explained by possible imperfections in the aperture and orbit, the incomplete spatial coverage of the BLMs, and the fact that the BLMs detect the showers on the outside of the magnets, downstream of the actual impact position.

## ALLEVIATION OF BFPP LOSSES AT LHCb

Since the installation of new TCLD collimators is not possible in the short term, a partial mitigation of BFPP losses from IP8 by means of an orbit bump has been investigated. For both B1 and B2, an horizontal orbit bump ( $-5.3$  mm on MQML.10R8.B1 and  $+5$  mm on MQML.10L8.B2) has been matched with MAD-X to make the BFPP beam miss

Table 1: RMS Longitudinal Extension ( $\sigma$ ) of Loss Patterns Given by BFPP Beams without and with Orbit Bumps for Different Values of Emittance and Energy

	without orbit bump (cell 10)				with orbit bump (cell 12)			
	B1 ( $s = 386.4$ m)		B2 ( $s = 365.3$ m)		B1 ( $s = 490.6$ m)		B2 ( $s = 468.7$ m)	
Normalized emittance	1.6 $\mu\text{m}$	2.3 $\mu\text{m}$	1.6 $\mu\text{m}$	2.3 $\mu\text{m}$	1.6 $\mu\text{m}$	2.3 $\mu\text{m}$	1.6 $\mu\text{m}$	2.3 $\mu\text{m}$
$\sigma$ at 6.37 Z TeV	0.234 m	0.281 m	0.315 m	0.379 m	1.383 m	1.657 m	1.256 m	1.507 m
$\sigma$ at 7 Z TeV	0.223 m	0.268 m	0.302 m	0.361 m	1.319 m	1.582 m	1.199 m	1.438 m

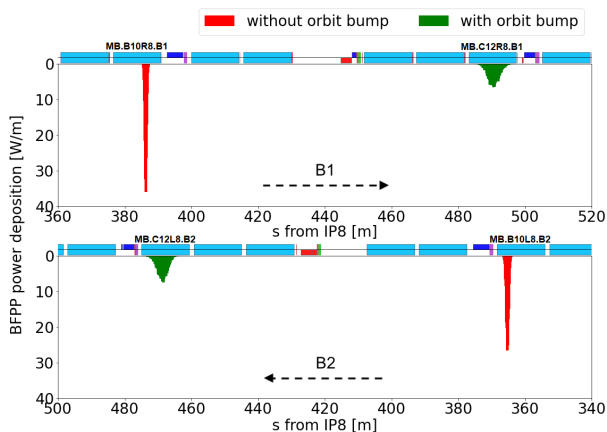


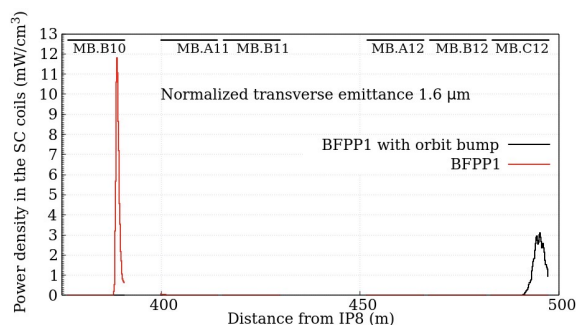
Figure 2: BFPP power deposition on MB.B10R8.B1 and MB.B10L8.B2 (without orbit bump) and on MB.C12R8.B1 and MB.C12L8.B2 (with orbit bump) for operating conditions of Pb-Pb 2018 run, simulated with SixTrack.

the first impact location of its dispersive trajectory in cell 10 and instead be lost in cell 12 (Fig. 1).

New loss patterns, simulated with SixTrack including the implemented orbit bumps, show losses shifted to 490.6 m and 468.7 m from IP8, in the superconducting dipoles MB.C12R8.B1 and MB.C12L8.B2 respectively. There the  $\beta$ -function is larger, and hence the transverse size of the BFPP beam is larger, meaning that the power deposition is more spread out. In addition, there is more margin in cell 12 due to higher beam abort thresholds [21]. The BFPP losses simulated for 2018 run, with and without orbit bump, are shown in Fig. 2. They are normalized to a power load in W/m for a levelled luminosity of  $10^{27} \text{ cm}^{-2} \text{ s}^{-1}$  and a BFPP cross section of 278 b. Also the RMS longitudinal sizes of the new loss distributions in the different cases are shown in Table 1, where the most critical ones are highlighted in red.

## FLUKA ENERGY DEPOSITION STUDY

The results of the discussed SixTrack simulations have been used as input to carry out a full energy deposition study with FLUKA [22–24], a multi-purpose particle-physics Monte Carlo simulation code. The power load on the superconductive coils of MB.B10R8.B1 and MB.C12R8.B1 have been estimated in the two scenarios, with and without orbit bump, at 6.37 Z TeV and for different transverse emittances, using a detailed 3D geometry. A qualitatively similar

Figure 3: BFPP power deposition simulated by FLUKA, for a luminosity of  $10^{27} \text{ cm}^{-2} \text{ s}^{-1}$  and a normalized emittance of  $1.6 \mu\text{m}$ .

situation is expected at higher beam energies, although the impact distribution is slightly narrower due to the smaller beam size (see Table 1).

From the most critical studied normalized emittance of  $1.6 \mu\text{m}$ , the simulated maximum radially averaged power density in the superconducting coil of the impacted magnet is  $\sim 12 \text{ mW/cm}^3$  without bump and  $\sim 3 \text{ mW/cm}^3$  with the orbit bump (Fig. 3). This confirms that the partial alleviation of BFPP losses around IP8 through orbit bumps would be possible. Given that the quench limit is estimated to be  $15\text{--}20 \text{ mW/cm}^3$  [8], the levelled luminosity at LHCb can be safely increased by at least a factor 2–3 in future runs.

## CONCLUSION

BFPP in Pb-Pb collisions is the most significant process in terms of localised beam losses. It imposes luminosity limitations due to the risk of quenching impacted magnets. BFPP losses were previously studied and mitigations have been proposed for all LHC experiments except LHCb, for which a higher luminosity has been requested in future runs. A full study of BFPP losses during Pb-Pb collisions at IP8 has been carried out. The loss patterns caused by BFPP particles from IP8 have been simulated with SixTrack and compared to measured BLM signals. A partial mitigation of these losses has been proposed, by shifting them through an orbit bump from cell 10 to cell 12, where they are more spread out and cause a lower peak power load. This has been confirmed by energy deposition studies realized with FLUKA. The proposed orbit bump would allow to increase LHCb luminosity by a factor 2–3 in future Pb-Pb runs, without the installation of new hardware.

## REFERENCES

- [1] O. S. Brüning *et al.*, “LHC design report v.1 : The LHC main ring,” *CERN-2004-003-VI*, CERN, Geneva, Switzerland, 2004. <https://cds.cern.ch/record/782076>
- [2] J. M. Jowett *et al.*, “First Run of the LHC as a Heavy-ion Collider,” in *Proc. IPAC’11*, San Sebastian, Spain, 2011, pp. 1837–1839. <https://jacow.org/IPAC2011/papers/TUPZ016.pdf>
- [3] J. M. Jowett *et al.*, “The 2015 Heavy-Ion Run of the LHC,” in *Proc. IPAC’16*, Busan, Korea, 2016, pp. 1493–1496. doi:10.18429/JACoW-IPAC2016-TUPMW027
- [4] J. M. Jowett, “Colliding Heavy Ions in the LHC,” in *Proc. IPAC’18*, Vancouver, Canada, 2018, pp. 584–589. doi:10.18429/JACoW-IPAC2018-TUXGBD2
- [5] J. M. Jowett *et al.*, “The 2018 Heavy-Ion Run of the LHC,” in *Proc. IPAC’19*, Melbourne, Australia, 2019, pp. 2258–2261. doi:10.18429/JACoW-IPAC2019-WEYYPLM2
- [6] R. Bruce *et al.*, “HL-LHC operational scenario for Pb-Pb and p-Pb operation,” *CERN-ACC-2020-0011*, 2020. <https://cds.cern.ch/record/2722753>
- [7] R. Bruce, M. Jebramcik, J. Jowett, T. Mertens, and M. Schaumann, “Performance and luminosity models for heavy-ion operation at the CERN Large Hadron Collider,” *Eur. Phys. J. Plus*, vol. 136, p. 745, 2021. doi:10.1140/epjp/s13360-021-01685-5
- [8] M. Schaumann, J. M. Jowett, C. Bahamonde Castro, R. Bruce, A. Lechner, and T. Mertens, “Bound-free pair production from nuclear collisions and the steady-state quench limit of the main dipole magnets of the CERN Large Hadron Collider,” *Phys. Rev. Accel. Beams*, vol. 23, p. 121 003, 2020. doi:10.1103/PhysRevAccelBeams.23.121003
- [9] S. R. Klein, “Localized beampipe heating due to e- capture and nuclear excitation in heavy ion colliders,” *Nucl. Inst. & Methods A*, vol. 459, p. 51, 2001. <https://cds.cern.ch/record/437561/files/0005032>
- [10] R. Bruce, D. Bocian, S. Gilardoni, and J. M. Jowett, “Beam losses from ultraperipheral nuclear collisions between Pb ions in the Large Hadron Collider and their alleviation,” *Phys. Rev. ST Accel. Beams*, vol. 12, no. 7, p. 071 002, 2009. doi:10.1103/PhysRevSTAB.12.071002
- [11] J. M. Jowett *et al.*, “The 2016 Proton-Nucleus Run of the LHC,” in *Proc. IPAC’17*, Copenhagen, Denmark, 2017, pp. 2071–2074. doi:10.18429/JACoW-IPAC2017-TUPVA014
- [12] J. M. Jowett *et al.*, “Overview of ion runs during Run 2,” *Proceedings of the 9th LHC Operations Evian Workshop, Evian, France*, 2019. <https://indico.cern.ch/event/751857/timetable/#20190130.detailed>
- [13] G. Apollinari *et al.*, *High-Luminosity Large Hadron Collider (HL-LHC): Technical Design Report V. 0.1*. CERN, Geneva, Switzerland, 2017. doi:http://dx.doi.org/10.23731/CYRM-2017-004
- [14] R. Bruce, “Outcome of LHC Pb beam tests at 6.8 Z TeV,” *presented at the 14th Int. Particle Accelerator Conf. (IPAC’23), Venice, Italy, 2023, paper MOPL021, this conference*, 2023.
- [15] *MAD-X program*, <http://cern.ch/mad/> CERN, Geneva, Switzerland.
- [16] F. Schmidt, “SixTrack. User’s Reference Manual,” *CERN/SL/94-56-AP*, CERN, Geneva, Switzerland, 1994.
- [17] G. Robert-Demolaize, R. W. Assmann, S. Redaelli, and F. Schmidt, “A New Version of SixTrack with Collimation and Aperture Interface,” in *Proc. PAC’05*, Knoxville, TN, USA, 2005, pp. 4084–4086. <https://jacow.org/p05/papers/FPAT081.pdf>
- [18] R. Bruce *et al.*, “Simulations and measurements of beam loss patterns at the CERN Large Hadron Collider,” *Phys. Rev. ST Accel. Beams*, vol. 17, p. 081 004, 2014. doi:10.1103/PhysRevSTAB.17.081004
- [19] *Sixtrack web site*, <http://sixtrack.web.cern.ch/SixTrack/>.
- [20] J. Wenninger, “Operation and Configuration of the LHC in Run 2,” *CERN-ACC-NOTE-2019-0007*, 2019. <http://cds.cern.ch/record/2668326>
- [21] A. Lechner *et al.*, “BLM Thresholds and UFOs,” 209–214. 6 p, 2017. <https://cds.cern.ch/record/2293680>
- [22] CERN, *Fluka website*, <https://fluka.cern>.
- [23] C. Ahdida, D. Bozzato, D. Calzolari, F. Cerutti, N. Charitonidis, A. Cimmino, *et al.*, “New Capabilities of the FLUKA Multi-Purpose Code,” *Frontiers in Physics*, vol. 9, 2022. doi:10.3389/fphy.2021.788253
- [24] G. Battistoni, T. Boehlen, F. Cerutti, P. W. Chin, L. S. Esposito, A. Fassò, *et al.*, “Overview of the FLUKA code,” *Ann. Nucl. Energy*, vol. 82, 10–18. 9 p, 2015. doi:10.1016/j.anucene.2014.11.007